

STUDY ON THE PERFORMANCE OF [PAC/PSf]-MIXED MATRIX MEMBRANE USED IN WATER FILTRATION

Ștefan Cătălin PINTILIE*, Laurenția Geanina PINTILIE,
Andreea Liliana LAZĂR, Ștefan BALTĂ

"Dunarea de Jos" University of Galati, Romania
e-mail: stefan.pintilie@ugal.ro

ABSTRACT

The polysulfone used in membrane manufacturing showed low performances in wastewater treatment when compared with other special polymers. Researchers worldwide are trying to improve membrane performances through different techniques, such as: blending, grafting and surface chemical reaction, etc. [1]. Blending is an efficient technique with great performance and relative low cost compared with other means of membrane enhancement. All membranes were manufactured by phase inversion and the composite membrane solution was mixed with powdered activated carbon (AC). The activated carbon is used on a large scale in conventional wastewater treatment systems, having good antibacterial properties and high absorption degree of contaminants. The studied membranes were characterized as follows: flux, permeability, retention of Naphthol Green B (NGB) dye, contact angle and SEM microscopy. The permeability results of the composite membranes blended with activate carbon particles showed better performance than the neat membrane, with an increase of 15.384%. Contact angle increased after powdered activated carbon blending in membrane matrix.

KEYWORDS: Polysulfone, Activated Carbon, Membrane, Retention, Flux, Permeability

1. Introduction

Water pollution is one of the major environmental problems in the world. Many techniques methods are used for the treatment of polluted water, such as precipitation by chemical agent, adsorption on activated carbon, membrane processes (microfiltration, ultrafiltration, nanofiltration, reverse osmosis), etc. [1, 2].

Separation based membranes are suitable in many industries, such as the chemical [3], food and pharmaceutical industries [4], possessing important advantages, such as no by-product production, low temperature process and an exceptional cost/efficiency ratio [5, 6].

Research in this area is increasing in order to continually optimize membrane performance [7, 8]. Increasing separation yield [7] and membrane flux [8] have been the target of many of these investigations [9]. A favourable scenario would be the possibility of increasing the membrane flux and its altogether separation [10].

Composite membranes have gained interest in research because of their combining at the same time properties of both polymer and filler.

Activated carbon (AC) is considered an important material, which is commonly used in water treatment activities.

The groups of organics that are generally adsorbed onto the activated carbon include pesticides, herbicides, aromatic solvents, polynuclear aromatics, chlorinated aromatics, soluble organic dyes, among more others [11]. Similar with nanoparticles, active carbon exhibits an extended surface area with a high degree of porosity [12]. AC is understood as a type of processed carbon particles with nano-micro volumes, meaning a high porosity, that results in a very high surface area (e.g. 500 m²). For the activation of carbon particles, chemical treatments are often required for their good adsorption properties [13].

Activated carbon-blended membranes used for the experiments described in this article attest an enhancement in terms of permeability and retention.

As far as the authors knowledge is concerned, the attempt to blend activated carbon particles

directly into the polymer matrix of a membrane has not been approached in literature.

2. Materials and methods

2.1. Materials

The polymer is polysulfone (PSf, average Mw~35000), the solvent is n-methylpyrrolidone (NMP, C₅H₉NO, 99%), both chemicals being purchased from Sigma-Aldrich.

Purchased from local provider, the activated carbon (AC) was in initial form of granules (GAC),

with an average granule size of 1.948 mm, requiring a decrease in size so that it could be mixed in the polymer solution.

2.2. Powdered activated carbon (PAC) preparation

Due to their very large granular size, as shown in Figure 1.a, the GAC particles were being continuously ground (for 3 h) to decrease the size of the particles (Figure 1.b), and then they were mesh sieved, in order to eliminate the particles larger than 100 μm.

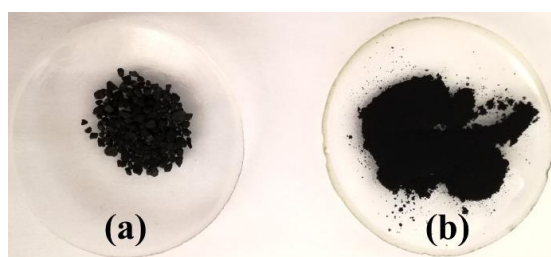


Fig. 1. Activated carbon in form of: a) granules (GAC) and b) powder (PAC)

The particle morphology and absorption capacity of NGB dye differences between GAC and PAC particles will be discussed.

2.3. Membrane preparation

The membranes referred to in this study were obtained by phase inversion, the immersion precipitation method.

The neat membrane casting solution was prepared by mixing the PSf polymer (25 wt%) with an NMP solvent solution at a constant temperature and under continuous stirring. For a homogeneous casting solution (Figure 2.a), stirring was being made for at least 24 h.

The AC blended membranes were prepared by adding 0.1 wt% of powdered activated carbon (PAC) in the corresponding volume of NMP for 1 h through continuous stirring at room temperature. The polymer was then added to the solution and stirring was made for at least 24 h (Figure 2.b).

After 24 h, the polymer solution was cast with 250 μm thickness using a film applicator (Automatic Film Applicator PA-2101, BYC-Gardner GmbH) on a very porous polyester as support layer. The casted solution was immersed in a distilled water bath in order to start the phase inversion process.

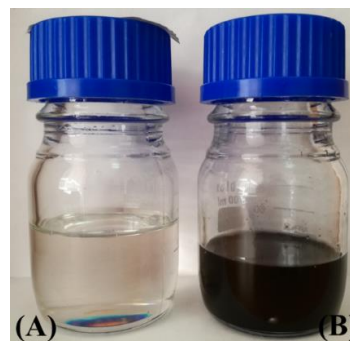


Fig. 2. Membrane solution after 24 h of continuous stirring for (A) neat PSf and (B) PSf blended with 0.1 wt% PAC

Table 1. Membrane characterization by concentrations

Membrane	PSf concentration [wt%]	PAC concentration [wt%]
Neat_PSf	25	-
PSf_0.1_AC	25	0.1

The resulting membranes (Table 1) were washed with distilled water and stored wet, until they were used as samples for characterization.

3. Characterization methods for membranes and activated carbon powder

3.1. SEM analysis

Sample surface and particle morphologies were investigated using the FEI Quanta 200 Scanning Electron Microscope, after coating with gold by sputtering.

3.2. Characterization of GAC and PAC particles

The size and distribution of activated carbon particles (GAC and PAC) were estimated from SEM images using ImageJ software (<https://imagej.nih.gov/ij/>). An example of ImageJ software particle analysis is shown in Figure 3.

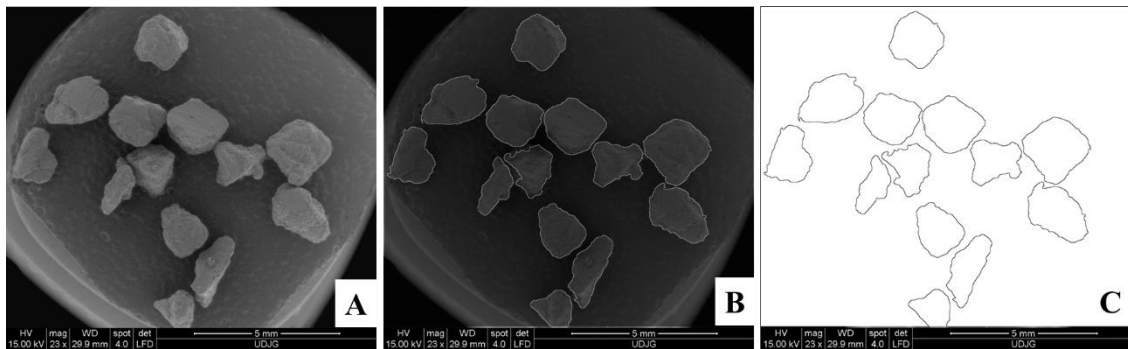


Fig. 3. Steps in identifying and analysing particles using ImageJ software: (A) SEM image as received uploaded in the software; (B) Particle identification; (C) Background subtraction for a clearer understanding of particle form

For a precise determination of activated carbon particle size, a number of 500 particles (for PAC) and 100 particles (for GAC) were measured in terms of circularity, with the Heywood diameter and Feret’s diameter (Table 2).

The size of GAC and PAC particles were determined through two widely used methods: the first method was by assuming that the AC particles were perfect spheres, method known as the Heywood diameter, thus finding the diameter with the following equation [14-17]:

$$A = \pi r^2 \quad (1)$$

where A is the particle area, the number π is a mathematical constant and r is the radius of the theoretic-spherical particle.

The Feret’s diameter was used as a second measuring method, defined as the distance between two opposite parallel tangents of a particle image, as presented in Figure 4 [14, 16, 17].

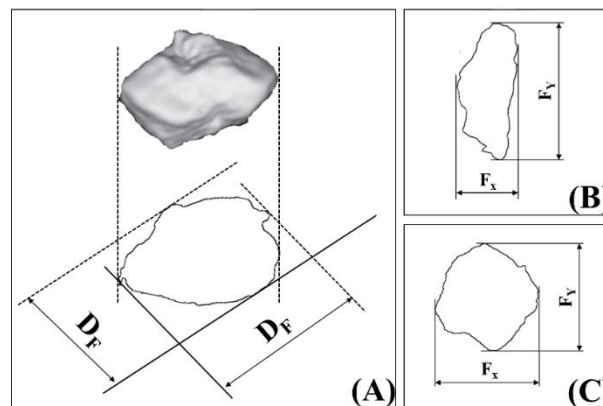


Fig. 4. Example of particle size analysis with Feret’s diameter: (A) 3D projection of a particle; (B) illustration of horizontal (F_x) and (C) vertical (F_y) Feret’s diameters of a particle

The projection from 3D object on a 2D plane is often used as a measuring technique in particle size analysis [15, 16].

3.2. Contact angle measurements

The hydrophilicity/hydrophobicity property of the samples was evaluated using a goniometer (OCA 15EC, DataPhysics), consisting in the measurements of contact angle between a water drop and the studied membrane surface.

3.3. Permeation tests

All permeation tests (pure water flux, permeability, retention, relative flux and relative flux reduction) were conducted in a dead-end stirred cell (Sterlitech HP4750) with 300 mL total volume and membrane surface area of 14.6 cm². The cell is connected to a nitrogen tank in order to create pressure for the liquid to be forced through the membrane.

Pure water flux J_0 (L/m² h) was measured using the gravimetric method and was determined by:

$$J_0 = \frac{V}{A \cdot t} \quad (2)$$

where V is the volume of the permeate water (L), A is membrane effective area (m²) and t is permeation time (h).

Water permeability experiments were carried out with pure water at operating pressures ranging between 6 and 12 bar at room temperature (approx. 25 °C).

The slope of the linear regression of J_0 on Δp was determined as the pure water permeability P_w (L/m² h bar), which was calculated using the following expression:

$$P_w = \frac{J_0}{\Delta p} \quad (3)$$

where Δp is the operating pressure (bar).

3.4. Retention tests

The dye of choice is NGB. It is a green nitroso dye used for industry purposes, such as staining wool, nylon, paper, anoxidized aluminum and soap manufacturing [18]. The molecular weight of NGB dye is 878.45 g/mol.

The NGB dye rejection ratio was calculated by the following equation:

$$Retention [\%] = \left(1 - \frac{C_f}{C_0}\right) \times 100 \quad (4)$$

where C_0 represents dye concentrations in feed solution (100 ppm) and C_f is the permeate concentration. Concentrations were determined spectroscopically using HACH DR 5000 UV-Vis Spectrophotometer (Hach, Germany) device.

3.5. Relative flux

Fouling is evaluated with a relationship of relative flux, which is the ratio of retention flux of NGB dye at any time during the fouling test to the initial flux, calculated with the following equation:

$$RF = \frac{J_r}{J_0} \quad (5)$$

The retention flux J_r [L/m² h] is similar with the pure water flux, except that feed subjected to filtering is NGB dye solution of 100 ppm.

In literature, in order for a membrane to have high anti-fouling properties, the relative flux must tend to value 1. If the relative flux tends more towards the value 0, the membrane is rapidly fouling, thus decreasing the production filtered water [19-22].

3.6. Relative flux reduction

The Relative flux reduction, RFR, is calculated as follows:

$$RFR = \left(1 - \frac{J_r}{J_w}\right) \times 100 \quad (6)$$

In simple terms, the RFR method shows how much fouling occurred at the end of filtration.

4. Results and discussions

4.1. Morphology of GAC and PAC particles and NGB dye absorption capacity

The Electron microscopy is a direct method described in the standards approved by ISO [23] and recognized by Health Agencies to perform size measurements and particle size distribution [17].

As shown in Figure 5.a, the GAC particles are of different sizes and irregular shapes, with an average circularity of less than 0.8 (Table 2).

After grinding the GAC particles, the size is reduced considerably, obtaining fine and very fine particles of activated carbon (Figure 5.b and 5.c).

Figure 6 represents the particle size distribution for GAC and PAC particles.

The size distribution of GAC particles (Figure 6.A) is in the range of 1000-3000 μm , with an

average Feret's diameter of 1948.585 μm (1.948 mm).

When analysing the size distribution of PAC particles, Figure 6.B, it can be seen that most counts were in the 0-20 μm interval, with over 400 counts

out of 500. Magnifying the graph to the 0-10 μm interval, 56% of the total numbered particles are less than 2 μm in size, meaning that the grinding process was effective, as it can be seen in Figure 5.b and Figure 5.c.

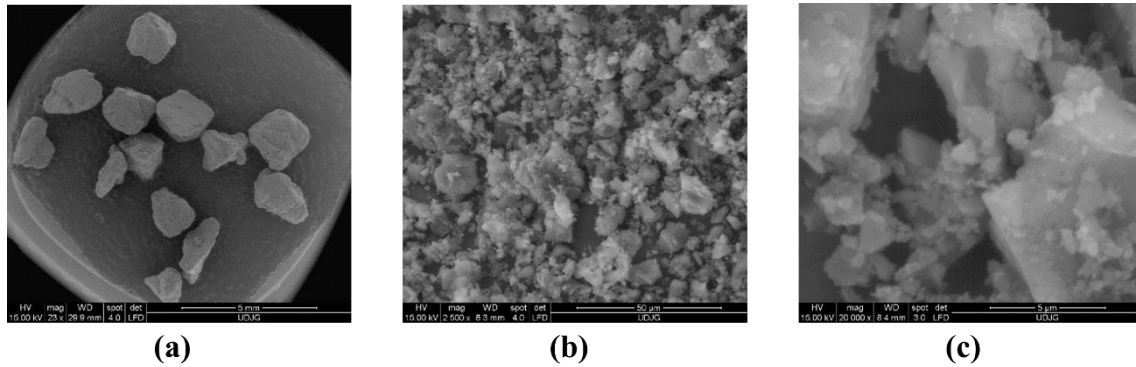


Fig. 5. SEM image for: (a) GAC particles, magnification 23X and PAC particles at two magnifications, (b) 2500X and (c) 20000X

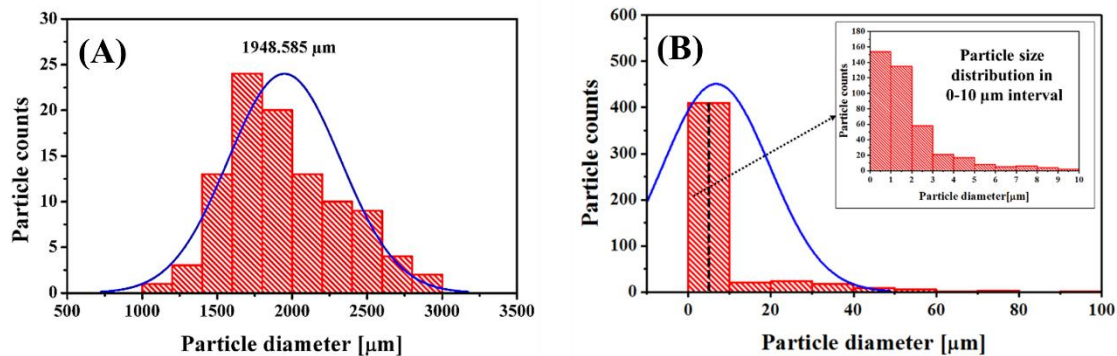


Fig. 6. Particle size distribution for (A) GAC particle and (B) PAC particles

Table 2. Total particle counts, sizes and circularity for GAC and PAC particles

Activated carbon form	Total particle counts	Heywood diameter [μm]	Feret's diameter [μm]	Circularity
GAC	100	1566.274	1948.585	0.798
PAC	500	6.661	8.565	0.784

According to the American Society for Testing and Materials (ASTM D5158), particle sizes of 0.177 mm (177 μm) and smaller are classified as powdered activated carbon with the acronym PAC [24].

Both the GAC and PAC particles maintain the same form, approved by the average circularity of both types (Table 2).

The size reduction of GAC particles after grinding was approximately equal for the two methods of diameter measuring, of approximately 99.5%, from 1948.585 μm to 8.565 μm , for Feret's diameter method, and from 1566.274 μm to 6.661 μm , for the Heywood diameter method, respectively.

The PAC/GAC ratios were similar for the Heywood diameter and Feret's diameter, at a value of 0.004.

Grinding the active carbon granules in order to reduce it to an acceptable size to be mixed in the polymer solution improved the performance of the active carbon in terms of NGB dye absorption. 0.1 g of both activated carbon forms were immersed in a 100 ppm dye solution for one day.

After one day it was observed that the activated carbon powder had absorbed 100 % of the dye solution, while the granulated activated carbon had absorbed only 67% (Figure 7), because of the low surface area which came in contact with the dye solution.

In general, decreasing the particle size leads to an increase in active surface area (m^2/g) [25, 26]. Higher surface area of the activated carbon increases the absorption capacity of dyes, evidenced by Figure

7. It is of great interest that the size of particles to be as small as possible.

Reducing the activated carbon particle size will lead to improved membrane performance.

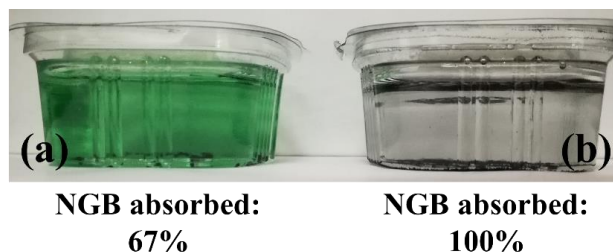


Fig. 7. Absorption of NGB dye after one day for: a) 0.1 g of activated carbon granules; b) 0.1 g of activated carbon powder

4.2. Membrane characterization with SEM observations

Figure 8 shows the influence of the activated carbon on the membrane surface morphology. Regarding the pore size, the neat membrane shows

larger, irregular shaped pores leading to low permeability and flux. Consequently, the decrease in pore size, due to activated carbon addition, the composite membrane will show a better retention of NGB.

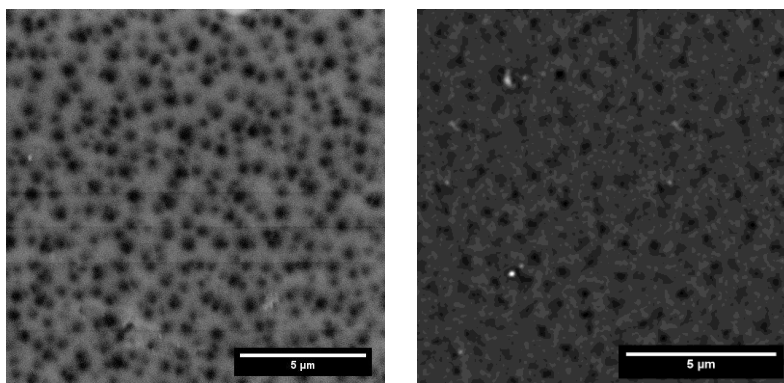


Fig. 8. Top-view SEM images of neat PSf membrane (left) and activated carbon-blended membrane (right)

4.3. Contact angle

The contact angle data of PSf-activated carbon membrane is shown in Table 3. The contact angle of the neat PSf membrane surface was lower compared to the AC-blended membrane. However, AC-blended membrane showed a higher water contact angle of

77.637°, which indicated that the activated carbon is hydrophobic, suggesting that the PAC particles changed the polarity of membrane surface from hydrophilicity to hydrophobicity. The hydrophobicity of the activated carbon is reported by other authors, also [27, 28].

Table 3. Contact angle, permeability, dye retention and relative flux reduction measurements of the studied membranes

Membrane	Contact angle [°]	Permeability [L/m ² h bar]	NGB dye retention [%]	RFR [%]
Neat_PSf	71.4	14.9	47.8	27.4
PSf_0.1_AC	77.6	15.5	56.8	22.2

Also, the contact angle measurement is a good criterion in approving the presence of activated carbon particles at membrane surface.

4.4. Permeation tests

Distilled water flux was determined by timing from 5 to 5 mL the filtered solution. Values are displayed in Figure 9 in order to study the membrane stability. The neat membrane shows an average flux of 149 L/m² h.

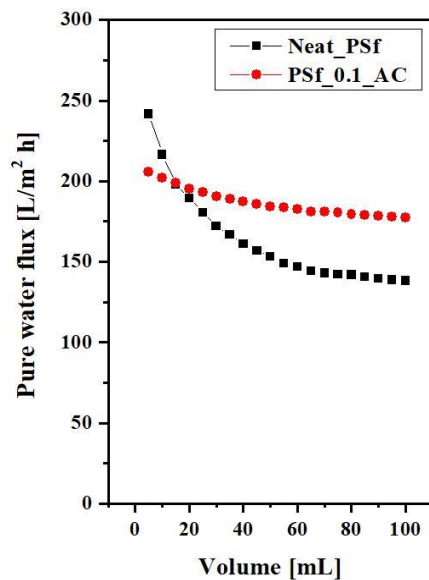


Fig. 9. Pure water flux for neat membrane and activated carbon blended membrane

Adding 0.1 wt% activated carbon powder in the membrane matrix increases the flux with 19%. Correlating the lower flux value with the top-view SEM images of the neat membrane, it appears that the irregularity in pore size distribution creates membrane instability over time. In terms of flux stability, the composite membrane displays a better result. Also, the composite membrane shows a 20.8% higher permeability than the neat membrane (Table 3). The retention is proportional with permeability, with an increase of 20.4% (Table 3).

The relative flux is usually used for the comparison of relative membrane antifouling performance [29, 30]. A high relative flux results in higher antifouling ability [31]. Low values (below 0.75) of relative flux indicated that neat polysulfone membranes have poor antifouling ability when comparing with the composite membrane (with a 0.78 relative flux value).

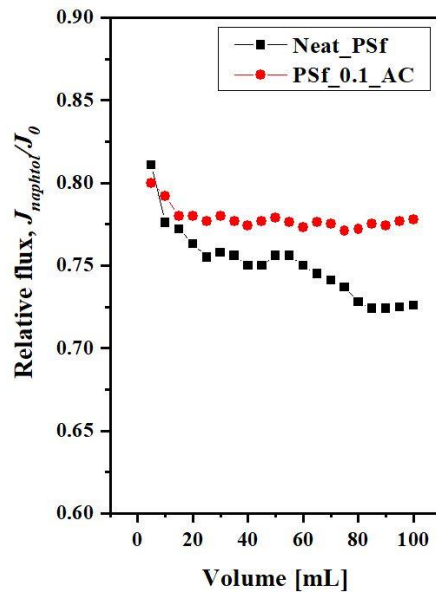


Fig. 10. Relative flux of pristine membrane and activated carbon composite membrane

The changing trends in the relative flux of membranes are shown in Figure 10 which demonstrates that the fouling resistance of modified membranes increases, when activated carbon is incorporated in the membrane. An explanation is the fact that the dye deposition on the membrane surface is lower because of the activated carbon ability to absorb dyes, thus cleaning the membrane’s surface during the filtration process.

4.5. Relative flux reduction

Table 3 shows the relative flux reduction of the membranes, also. The relative flux reduction is an important membrane investigation tool for the finding of the membrane with the lowest value, meaning that the respective membrane has the highest antifouling ability.

As expected, the neat PSf membrane shows the highest fouling with 27.4%, while the activated carbon blended membranes show a relative flux reduction of 22.2%.

5. Conclusions

The results of this research show that activated carbon particles at low concentration have a positive influence on the PSf membranes. The composite membrane exhibits better properties in terms of flux stability and flux (20.805 % increase), permeability (15.384% increase) and retention (20.408% increase). The presence of activated carbon in the membrane matrix increase the contact angle with 8.45%.

Although the relative flux reduction difference between the neat and composite membrane is low (5%), it is an acceptable proof that the activated carbon powder enhances membrane performances, even with its relatively larger size particles when compared with state-of-the-art nanoparticle blended membranes. Further research is required to determine the optimal concentration of activated carbon addition, but also a study on the influence of the activated carbon particle size in the polymeric membranes.

References

- [1]. Ng L. Y., Mohammad A. W., Leo C. P., Hilal N., *Polymeric membranes incorporated with metal/metal oxide nanoparticles: A comprehensive review*, Desalination, vol. 308, p. 15-33, 2013.
- [2]. Homayoonfal M., Akbari A., *Preparation of polysulfone nano-structured membrane for sulphate ions removal from water*, Iran. J. Environ. Health. Sci. Eng., vol. 7, no. 5, p. 407-412, 2010.
- [3]. Shirazi M. J. A., Bazgir S., Shirazi M. M. A., Ramakrishna S., *Coalescing filtration of oily wastewaters: characterization and application of thermal treated, electrospun polystyrene filters*, Desalin. Water Treat., vol. 51, no. 31-33, p. 5974-5986, 2013.
- [4]. Shirazi M. J. A., Kargari A., Tabatabaei M., Ismail A. F., Matsuura T., *Concentration of glycerol from dilute glycerol wastewater using sweeping gas membrane distillation*, Chem. Eng. Process. Process Intensif., vol. 78, p. 58-66, 2014.
- [5]. Baker R. W., *Membrane Technology and Applications*, 2nd ed. Menlo Park, California: John Wiley and Sons, 2004.
- [6]. Tiron L. G., Pintilie Ş. C., Vlad M., Birsan I. G., Baltă Ş., *Characterization of Polysulfone Membranes Prepared with Thermally Induced Phase Separation Technique*, IOP Conf. Ser. Mater. Sci. Eng., vol. 209, p. 12013, 2017.
- [7]. Hausmanns B. K. S., Laufenberg G., *Rejection of acetic acid and its improvement by combination with organic acids in dilute solutions using reverse osmosis*, J. Membr. Sci., vol. 104, no. (1-2), p. 95-98, 1996.
- [8]. Cath A. E. C. T. Y., Adams V. D., *Experimental study of desalination using direct contact membrane distillation: a new approach to flux enhancement*, J. Membr. Sci., vol. 228, no. 1, p. 5-16, 2004.
- [9]. Emadzadeh D., Lau W. J., Ismail A. F., *Synthesis of thin film nanocomposite forward osmosis membrane with enhancement in water flux without sacrificing salt rejection*, Desalination, vol. 330, p. 90-99, 2013.
- [10]. Chen X. N., Wan L. S., Wu Q. Y., Zhi S. H., Xu Z. K., *Mineralized polyacrylonitrile-based ultrafiltration membranes with improved water flux and rejection towards dye*, J. Membr. Sci., vol. 441, p. 112-119, 2013.
- [11]. Hendricks D. W., *Water Treatment Unit Processes: Physical and Chemical*, CRC Press, 2006.
- [12]. Ferhan Cecen O. A., *Activated Carbon for Water and Wastewater Treatment: Integration of Adsorption and Biological Treatment*, Weinheim, Germany: Wiley-VCH Verlag GmbH & Co. KGaA, 2011.
- [13]. Manasi Ghamande S. G., Sacchidanand Gogawale, *Processed Waste to Process Waste*, Int. J. Adv. Res. Educ. Technol., vol. 3, no. 2, p. 65-69, 2016.
- [14]. Merkus H. G., *Particle Size Measurements: Fundamentals, Practice, Quality*, 2009.
- [15]. Pabst E., Gregorová W., *Characterization of particles and particle systems*, ICT Prague, p. 27-28, 2007.
- [16]. Arai Y., Akers R. J., Treasure C. R. G., *Chemistry of powder production*, vol. 1, English, 1996.
- [17]. Varenne F., Makky A., Gaucher-Delmas M., Violleau F., Vauthier C., *Multimodal Dispersion of Nanoparticles: A Comprehensive Evaluation of Size Distribution with 9 Size Measurement Methods*, Pharm. Res., vol. 33, no. 5, p. 1220-1234, 2016.
- [18]. Kiernan R. W. H. J. A., *Conn's Biological Stains: A Handbook of Dyes, Stains and Fluorochromes for Use in Biology and Medicine 10th*, Taylor and Francis, 2002.
- [19]. Huang L., Zhao S., Wang Z., Wu J., Wang J., Wang S., *In situ immobilization of silver nanoparticles for improving permeability, antifouling and anti-bacterial properties of ultrafiltration membrane*, J. Membr. Sci., vol. 499, p. 269-281, 2016.
- [20]. Ahmad A. L., Majid M. A., Ooi B. S., *Functionalized PSf/SiO₂ nanocomposite membrane for oil-in-water emulsion separation*, Desalination, vol. 268, no. 1-3, p. 266-269, 2011.
- [21]. Wang J., Sun H., Gao X., Gao C., *Enhancing antibiofouling performance of Polysulfone (PSf) membrane by photo-grafting of capsaicin derivative and acrylic acid*, Appl. Surf. Sci., vol. 317, p. 210-219, 2014.
- [22]. Zhang G., Lu S., Zhang L., Meng Q., Shen C., Zhang J., *Novel polysulfone hybrid ultrafiltration membrane prepared with TiO₂-g-HEMA and its antifouling characteristics*, J. Membr. Sci., vol. 436, p. 163-173, 2013.
- [23]. ***, *ISO/TS 10797:2012: Nanotechnologies - Characterization of single-wall carbon nanotubes using transmission electron microscopy*.
- [24]. Cheremisinoff N. P., *Perfluorinated Chemicals (PFCs): Contaminants of Concern*, 2016.
- [25]. Kallio T., *Antifouling properties of TiO₂: Photocatalytic decomposition and adhesion of fatty and rosin acids, sterols and lipophilic wood extractives*, Colloids Surfaces a Physicochem. Eng. Asp., vol. 291, no. 1-3, p. 162-176, 2006.
- [26]. Pintilie S. C., Tiron L. G., Birsan I. G., Ganea D., Balta S., *Influence of ZnO Nanoparticle Size and Concentration on the Polysulfone Membrane Performance*, Mater. Plast., vol. 54, no. 2, p. 257-261, 2017.
- [27]. Zhou W., Zhang P., Liu W., *Anatase TiO₂ nanospindle/activated carbon (AC) composite photocatalysts with enhanced activity in removal of organic contaminant*, Int. J. Photoenergy, vol. 2012, p. 28-30, 2012.
- [28]. Sun H., *Superhydrophobic activated carbon-coated sponges for separation and absorption*, Chem. Sus. Chem., vol. 6, no. 6, p. 1057-1062, 2013.
- [29]. Qin H. L. J. J., Cao Y. M., Li Y. Q., Li Y., Oo M. H., *Hollow fiber ultrafiltration membranes made from blends of PAN and PVP*, Sep. Purif. Technol., vol. 36, p. 149, 2004.
- [30]. Babu V. G. G. P. R., *Membrane characteristics as determinant in fouling of UF membranes*, Sep. Purif. Technol., vol. 24, p. 23, 2001.
- [31]. Huang Z. Q., Chen K., Li S. N., Yin X. T., Zhang Z., Xu H. T., *Effect of ferrosulfate content on the performances of polysulfone-ferrosulfate oxide ultrafiltration membranes*, J. Membr. Sci., vol. 315, no. 1-2, p. 164-171, 2008.